Vipin Kumar
Assistant Professor.

Michael VanderWel
Graduate Student.

John Weller
Graduate Student.

Department of Mechanical Engineering,
University of Washington,
Seattle, WA 98195

Karl A. Seeler
Assistant Professor,
Department of Mechanical Engineering,
Lafayette College,
Easton, PA 188042

Experimental Characterization of the Tensile Behavior of Microcellular Polycarbonate Foams

Novel polycarbonate (PC) foams with bubbles on the order of 10 μm and cell nucleation densities between 1 and 10 billion cells per cubic centimeter of foam have been produced using carbon dioxide as the blowing agent. The size and number of bubbles can be controlled to produce a wide range of foam densities. This paper presents the results of an experimental study of the tensile behavior of these unique microcellular foams. It was found that the tensile strength of microcellular PC foams is proportional to the foam density. The strength is less than that predicted by the rule of mixtures, suggesting that the microcellular structure is inefficient in carrying the tensile load. The saturation of PC by CO_2 was found to reduce the tensile strength of the virgin material by approximately 20 percent. This showed that the sorption of a very high concentration of gas molecules by the polymer must be considered when characterizing and modelling the microcellular foam mechanical properties. The relative tensile modulus of microcellular foam was found to increase as the square of the foam's relative density over the range of densities explored.

Introduction

Microcellular foams are polymeric foams with average cell sizes on the order of 10 μm. In addition to an extremely small cell size, microcellular plastics are also characterized by a very high cell nucleation density. Typically one hundred million or more bubbles are present in each cubic centimeter of material. Because a large number of cells are present, substantial reduction in density relative to the original material is possible. Microcellular plastics were originally conceived as a means to reduce the amount of material required to produce a part. The rationale behind their development was that if bubbles could be introduced to the polymer matrix which were smaller than the critical flaws inherent to the material then the density could be reduced without significantly affecting the mechanical properties.

A process to produce microcellular foams was developed by Martini et al. (1982, 1984) using a thermodynamic instability to cause bubble nucleation and growth. The process for producing the microcellular structure in thermoplastics, shown in Fig. 1, has two distinct stages. The first stage involves saturation of a sample with a non-reacting gas maintained at an elevated pressure and atmoshperic temperature. After an equilibrium amount of gas has been absorbed, the sample is returned to atmospheric pressure causing supersaturation. In the second stage of the process, the supersaturated sample is heated to a temperature near the glass transition temperature of the polymer. Because the polymer is plasticized by the absorbed gas, the glass transition temperature of the supersaturated sample is lower than that of the original, unsaturated polymer (Kumar and Weller, 1993). Heating the supersaturated sample increases the mobility of the polymer, allowing bubble nucleation and growth to occur.

The initial work on microcellular foams was performed on the polystyrene-nitrogen system. Colton and Suh (1987a,b) explored the nucleation phenomena in this system when varying concentrations of nucleating agents were introduced to the polymer. Kumar (1988) and Kumar and Suh (1990) explored the effect of the process parameters on the resulting microstructure of microcellular polystyrene, and developed an uncoupled batch process to produce three dimensional parts.

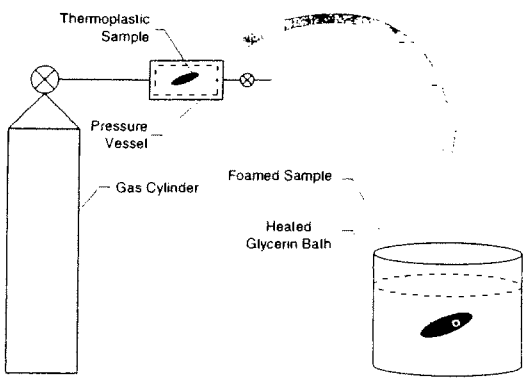

Fig. 1 Schematic of the microcellular foaming process

Contributed by the Materials Division for publication in the JOURNAL OF ENGINEERING MATERIALS AND TECHNOLOGY. Manuscript received by the Materials Division March 31, 1993. Associate Technical Editor: V. Stokes.

Table 1 Processing conditions for control specimens

Sample	Bath temperature (°C)	Immersion time (s)	CO_2 Saturation pressure (MPa)	CO_2 Desorption time (hours)*	ASTM specimen type	Number of specimens tested
control-1	None	None	None	N/A	IV	5
control-2	None	None	5.52	360	IV	5
control-3	60	30	None	N/A	IV	5
	80	30	None	N/A	IV	5
	100	30	None	N/A	IV	5
	120	30	None	N/A	IV	5
	140	30	None	N/A	IV	5
	160	30	None	N/A	IV	5
	180	30	None	N/A	IV	5

* After saturation with CO_2.

Recently, attention has been focused on other systems including poly (ethylene terephthalate) (Baldwin and Suh, 1992; Kumar and Gebizlioglu, 1991), high impact polystyrene (Kweeder et al., 1991; Ramesh et al., 1992), poly(vinylchloride) (Kumar and Weller, 1993) and polycarbonate (Kumar and Weller, 1991).

It is possible to create an unfoamed, integral skin of desired thickness on microcellular foams by allowing the gas to escape from the surface layers prior to heating of the specimen (Kumar and Weller, 1992). This control of skin thickness makes it possible to produce desired skin-core morphologies, thus providing additional flexibility to the engineer. By varying the gas saturation pressure and the foaming temperature, it is usually possible to create microcellular foams with a wide range of densities. In polycarbonate, for example, microcellular foams with densities ranging from 10 to 99 percent of the solid polycarbonate density have been produced (Kumar and Weller, 1991).

Since their inception some ten years ago, the primary emphasis in microcellular foam research has been on processing technology. Therefore, there is a general lack of data in the literature on the mechanical properties of these novel materials. This paper presents the first systematic investigation in the area of mechanical behavior of microcellular foams, and presents experimental results on the tensile behavior of microcellular polycarbonate of various densities.

Experimental

Sheets of Lexan 9030 polycarbonate, 1.5 mm thick, were used in the experiments. ASTM D638 type IV and type V specimens where cut from the sheets with gage lengths of 25.4 mm (1.00 in) and 7.62 mm (0.30 in) respectively. The tensile specimens were saturated in a pressure vessel with CO_2 gas maintained at an average pressure of 5.52 MPa (800 psi) and 22°C. The pressure was controlled to ±6 percent by a single stage regulator attached to a CO_2 cylinder. The saturation time for the specimens used in this experiment was 60 hours (Kumar and Weller, 1991), resulting in an equilibrium gas concentration of 112 mg CO_2 per gram of PC. Desorption tests conducted at room temperature and atmospheric pressure indicated that less than 1 percent of the gas remains dissolved in the specimens after 14 days (336 hours).

Table 2 Processing conditions for foamed specimens (all specimens were saturated with CO_2 at 5.52 MPa for 60 hours and allowed to desorb for 30 min before foaming)

Sample	Foaming temperature (°C)	Foaming time (s)	ASTM specimen type*	Number of specimens tested
B	60	30	IV	3
C	80	30	IV	5
D	100	30	IV	5
E	120	30	IV	5
F	140	30	IV	5
G	160	30	V	5
H	180	20	V	5

* Prior to foaming.

Upon saturation, the samples were removed from the pressure vessel and allowed to desorb CO_2 gas for 30 minutes. The samples were then foamed in a heated glycerin bath. The temperature used to foam the samples and the length of time the samples were held at this temperature will be referred to as the foaming temperature and immersion time respectively. This procedure produced an unfoamed skin of approximately 50 μm thick on the foamed specimens (Kumar and Weller, 1992). After foaming, the samples were quenched in water at room temperature. Tables 1 and 2 give the processing conditions used to produce the specimens for the experiments. Figure 2 shows a photograph of microcellular PC tensile specimens of

Nomenclature

E_f = modulus of the foam, MPa
E_m = modulus of the matrix, MPa
$E_{\text{control-1}}$ = modulus of the original, unprocessed material, MPa
$E_{\text{control-2}}$ = modulus of the saturation cycled, but unfoamed PC (control-2), MPa
ρ_f = density of the foam, g/cm^3
ρ_m = density of the matrix material, g/cm^3
$\rho_{\text{control-1}}$ = density of the original, unprocessed PC (control-1), g/cm^3
$\rho_{\text{control-2}}$ = density of the saturation cycled, but unfoamed PC (control-2), g/cm^3
$S_{y,f}$ = stress at yield of the foam, MPa
$S_{y,m}$ = stress at yield of the matrix material, MPa
$S_{y,\text{control-1}}$ = stress at yield of the original, unprocessed PC (control-1), MPa
$S_{y,\text{control-2}}$ = stress at yield of the saturation cycled, but unfoamed PC (control-2), MPa
$S_{b,f}$ = stress at break of the foam, MPa
$S_{b,m}$ = stress at break of the matrix material, MPa
$S_{b,\text{control-1}}$ = stress at break of the original, unprocessed PC (control-1), MPa
$S_{b,\text{control-2}}$ = stress at break of the saturation cycled, but unfoamed PC (control-2), MPa
$\%El_{b,f}$ = percent elongation at break of the foam
$\%El_{b,m}$ = percent elongation at break of the matrix
$\%El_{b,\text{control-1}}$ = percent elongation at break of the original, unprocessed PC (control-1)
$\%El_{b,\text{control-2}}$ = percent elongation at break of the saturation cycled, but unfoamed PC (control-2)

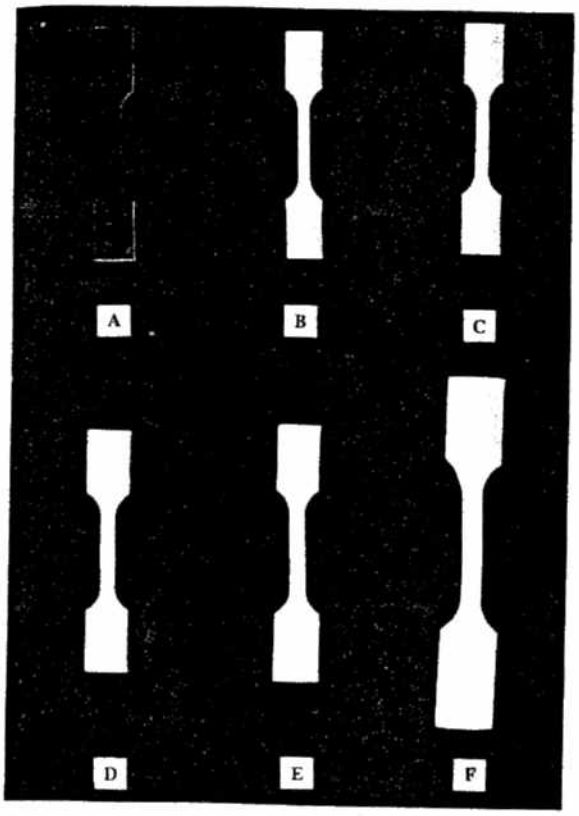

Fig. 2 Photographs of tensile specimens showing the change in dimensions after foaming

several densities, showing the relative changes in dimensions due to foaming, and Table 3 lists the average dimensions of the gage section of the samples after foaming. Although the specimens tested in this study had non-ASTM dimensions, the uniform foaming provided a constant thickness-to-width-ratio, and thus any size effects were deemed negligible. All specimens were aged at room temperature and atmospheric pressure for at least 360 hours prior to testing, allowing CO_2 remaining in the samples after foaming to escape from the polymer matrix.

The specimens were tested in tension using an Instron 4505 tensile testing machine and an extensometer with a 25.4 mm (1.0 in. gage length. All specimens were tested using a constant crosshead rate of 10.0 mm/min (0.39 in./min), corresponding to an approximate strain rate of 0.39 mm/mm/min. Five samples were tested at each density, generating five stress-strain curves. The stress reported in this paper is defined as the applied load divided by the original cross-sectional area of the gage section. The strain, unless otherwise noted, is defined as the change in length of the gage section divided by the original length of the gage section. Thus both the stress and strain will be referred to as "engineering stress" and engineering strain" respectively. The tensile modulus was determined by running a least squares fit through the initial linear portion of the engineering stress-strain curve. Further, the yield point will be defined as the first point where the engineering stress-strain curve has a slope equal to zero; this point has been shown to correspond to the first onset of permanent deformation in solid polymers (Brown, 1986), and is consistent with the definition set forth in ASTM standarized test method D-638. All tests were carried out at an ambient relative humidity of 48.0 ±5 percent and a temperature of 22°C. The density of the gage section was determined using the weight displacement method (ASTM D792), and the average cell size and cell density were determined from SEM micrographs using a procedure described previously (Kumar and Suh, 1990). The cell density

Table 3 Gage section dimensions prior to testing

Sample	Average thickness (mm)	Average width of gage section (mm)
A (control-1)	1.50	6.32
B	1.64	6.39
C	1.90	6.50
D	2.07	6.97
E	2.21	7.53
F	2.60	9.19
G	2.80	5.60
H	3.30	6.28

reported is the number of bubbles nucleated per unit volume of solid polymer, and is obtained by dividing the number of bubbles per cm^3 of foam by the foam void fraction.

Results and Discussion

The process outlined above produces microcellular foams with an integral skin surrounding an extremely uniform microcellular core. The foam core region can be divided into two parts: a uniform region and a transition region. The uniform region has a constant cell density and average bubble diameter, and thus the density of this region is also constant. The average cell diameters and cell densities reported in this paper were determined from micrographs taken of this region. For the desorption time of approximately 30 minutes used in this study, the uniform core region comprised about 80 percent of the cross-section. The skin region is of the order of 10μm, or about 1 percent of the cross-section. The transition region comprises the remaining one-fifth of the cross-section. In this transition region, the cell density increases from zero at the skin to the average cell density in the foam core. Bubbles are found to be larger near the skin, and they get smaller as we approach the uniform core region. The void fraction however, is found to be uniform throughout the entire foam cross-section (Kumar, 1988). Thus the density profile across the thickness varies from the solid polymer density in the skin to a lower but uniform density in the foamed region. As the skin thickness of the specimens in this study was of order of 1 percent of the specimen thickness, the effect of the skin on the tensile behavior of the foamed specimens was negligible.

It is customary in literature on cellular materials to normalize material properties such as strength and elastic modulus, etc., by the corresponding property for the solid matrix material that comprises the cell walls, and report the result as a "relative" property. This relative property is usually plotted as a function of the relative density of the cellular material, i.e., the density of the cellular material divided by the density of the solid that comprises the cell walls. In our characterization of microcellular foams, we were concerned about the effect of the microcellular process on the properties of the matrix—namely the gas sorption in the first stage of the process, and the exposure to a thermal cycle in the second stage of the process. To ascertain these effects, three kinds of control specimens were tested as described below.

Control-1 refers to the tensile specimens made from the PC sheets purchased. These specimens were neither saturated with CO_2 nor heated, and are also referred to as "virgin" material specimens or "unprocessed" specimens. These specimens were tested to establish the base-line tensile behavior of as-received PC. Control-2 specimens were saturated with 5.52 MPa (800 psi) CO_2, and then left at room temperature and pressure for at least 360 hours to let the CO_2 diffuse out of the specimens. The time required for complete desorption of CO_2 was determined from desorption experiments, in which specimens saturated at 5.52 MPa (800 psi) lost more than 99 percent of the absorbed gas in 340 hours. These specimens were tested to determine the permanent effect of saturating the polymer with

Table 4 Test results for control specimens

Sample	Foaming temp. (°C)	Density (g/cm³)	Tensile modulus (MPa)*	Tensile stress at yield (MPa)	Tensile stress at break (MPa)	% Elongation at break (%)
Control-1 virgin PC	None	1.2	2360 (43)**	64.9 (1.4)	73.2 (6.8)	131.4 (13.4)
Control-2 saturation cycled PC	None	1.2	2430 (250)	50.4 (0.3)	58.1 (3.2)	99.7 (9.1)
Control-3 thermal cycled PC	60	1.2	2150 (140)	67.2 (0.9)	70.2 (0.5)	144 (3.4)
	80	1.2	2100 (130)	65.7 (1.5)	61.5 (9.2)	106 (50)
	100	1.2	2100 (60)	66.3 (3.6)	61.9 (8.1)	115 (28)
	120	1.2	2000 (50)	66.0 (3.3)	62.4 (5.9)	106 (17)
	140	1.2	2050 (100)	65.3 (0.3)	61.4 (0.3)	108 (3.8)
	160	1.2	-	64.1 (0.6)	54.4 (6.0)	86.2 (42.6)
	180	1.2	-	64.4 (4.2)	63.9 (5.3)	143 (21.1)

* Modulus values were determined from engineering stress-strain curves where an extensometer was used.
** Values in parentheses are the standard deviation.

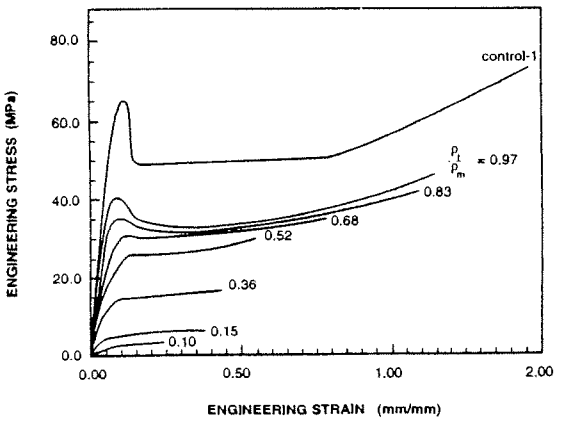

Fig. 3 Stress-strain curves for control-1 (original, unprocessed PC) and microcellular PC at different relative densities. The strain for this figure was estimated from the cross-head displacement.

CO_2 on the tensile behavior. Note that these specimens were not subjected to the thermal cycle used to create the microcellular foam, and are therefore referred to as "saturation cycle, but not foamed" specimens. The control-3 specimens were exposed to the thermal cycle used in the second stage of the microcellular process, but were not saturated with CO_2. Typically, the thermal cycle consists of heating the polymer in a glycerin bath at the foaming temperature for 30 s. The control-3 specimens were tested to determine the effect of the foaming thermal cycle on the matrix polymer properties.

Table 4 shows the tensile properties of the control specimens. There is a substantial drop in all of the tensile properties of the control-2 specimens, except the modulus. In addition, the ultimate properties of the control-2 specimens are approximately 20 percent below the properties of the control-1 material. These results are consistent with those of Chan (1978) and Chan and Paul (1979) except they reported a 5 and 8 percent increase in the ultimate tensile strength of 0.13 mm thick polycarbonate film specimens saturated in CO_2 at 4.1 and 6.1 MPa respectively and tested at an elongation rate of 25.4 mm/min. The discrepancy in the ultimate strength results could therefore be either a size or a strain rate effect. In contrast, tensile tests on the control-3 specimens show that the thermal cycle used to create microcellular foams does not affect the tensile properties of the original polymer.

Fig. 3 shows representative engineering stress-strain curves of unprocessed PC (control-1) and microcellular PC at several relative densities. It should be noted that only for this figure, the strain was determined from the displacement of the cross-heads and not the gage length. The strain for this figure was estimated from the cross-head displacement since the extensometer used in this study could not measure the deflection of the gage section up to the point of failure. All other strains computed in this paper are based on the deflection of an extensometer. Therefore, the strains in Fig. 3 are an underestimate of the actual strain in the gage section, and Fig. 3 only gives a qualitative indication of the effect of lowering the relative density on the tensile properties. During the tensile tests, necking was observed in the gage section of the control-1 and control-3 materials only. This necking occurred shortly after yield, and was not seen in the control-2 specimens or any of the microcellular foam specimens. Figure 3 shows that as the relative density decreases there are significant drops in the engineering stress at yield, engineering stress at break, and the elongation at break. These three parameters in turn affect the toughness and ductility of the material. Since the area under the engineering stress-strain curves decreases as the density decreases, the toughness also decreases. In addition, the shape of the engineering stress-strain curves changes with relative density. Above a relative density of approximately 0.50, there is a distinct hump at the yield point, a local maximum. Recall that the yield point in this paper was defined as the first point where the engineering stress-strain curve has a zero slope. For the foams with relative densities below 0.5, there is no distinct hump in the stress-strain curve and the yield definition cannot be applied. Finally, Fig. 3 shows that the tensile modulus drops as the relative density decreases.

Table 5 summarizes the experimental results from the tensile tests, lists the density of the gage section of the samples after foaming, and shows the average cell size and cell nucleation density of each foam. We note from Table 5 that the tensile strength at break is nearly equal to the tensile strength at yield for all of the relative densities explored. Figures 4 and 5 are plots of the tensile strength at break and the yield strength as a function of density for the microcellular PC, control-1, and control-2 specimens. The error bars represent one standard

Table 5 Experimental Results for PC foams

Sample	Density (g/cm^3)	Average cell diameter (μm)	Cell density (10^9 cells/cm^3)	Tensile modulus (MPa)	Tensile stress at yield (MPa)	Tensile stress at break (MPa)	% Elongation at break (%)
B	1.16	1.6	6.37	1780 (60)*	41.4 (0.3)	45.2 (6)	79 (19)
C	0.99	2.5	8.38	1470 (210)	34.0 (0.6)	40.6 (5.5)	83 (6)
D	0.82	3.6	6.48	1000 (110)	30.7 (0.5)	34.0 (1.9)	42 (9)
E	0.62	5.7	2.76	700 (120)	25.0 (0.4)	25.6 (5.5)	27 (28)
F	0.43	4.5	4.68	437 (110)	-	16.5 (1.3)	47 (6)
G	0.18	4.7	3.61	337 (130)	-	5.2 (0.6)	5.5 (2.5)
H	0.12	8.9	2.40	65 (23)	-	3.0 (0.4)	25 (5)

* The standard deviation is given in parentheses.

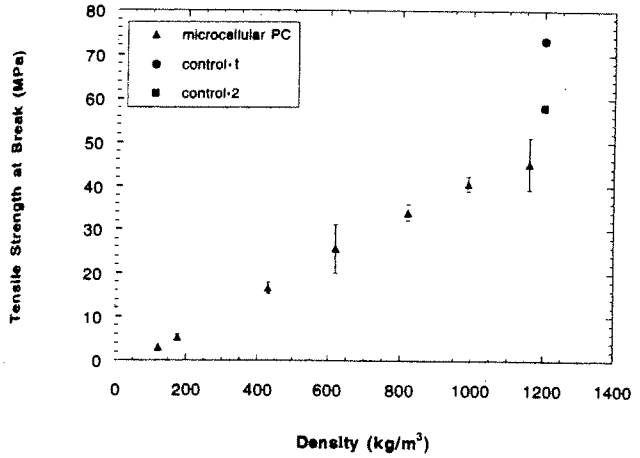

Fig. 4 Plot of the tensile strength at break of microcellular PC; original, unprocessed PC (control-1) and saturation cycled, but unfoamed PC (control-2) specimens as a function of density (1000 kg/m³ = 62.4 lb/ft³)

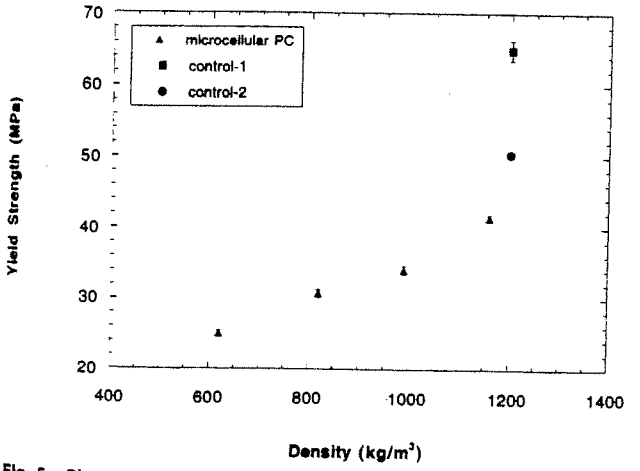

Fig. 5 Plot of the tensile yield strength of microcellular PC original, unprocessed PC (control-1) and saturation cycled, but unfoamed PC (control-2) specimens as a function of density (1000 kg/m³) = 62.4 lb/ft³)

deviation in the data. Both Figs. 4 and 5 illustrate the effect of CO_2 saturation cycling on the strength of the matrix material. There is a substantial drop in both the strength at break and the yield strength as indicated in Table 4. Further, the strength at break and the strength at yield of microcellular PC are directly proportional to the foam density.

Figure 6 is a plot of the relative tensile strength at break

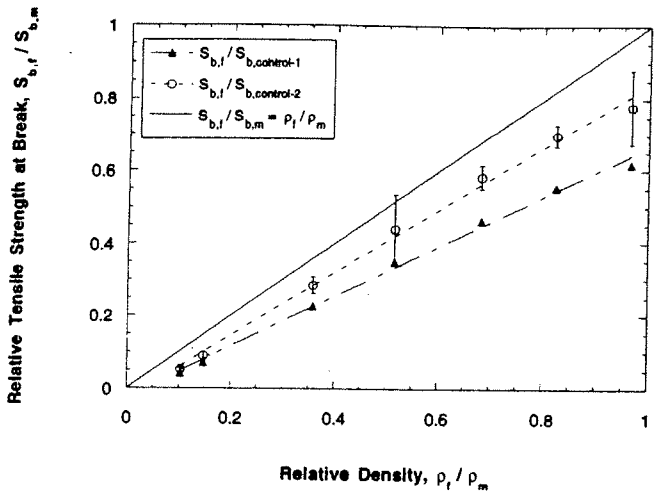

Fig. 6 Plot of the relative tensile strength at break of microcellular PC as a function of the relative density

normalized by the tensile strength of control-1 and control-2 specimens, and shows that the relative tensile strength is directly proportional to the foam relative density. For the sake of clarity, the error bars have been shown on the data normalized by control-1 properties only. The control-2 properties were also chosen to normalize the foam data since the control-2 properties are the best estimate of the foam matrix properties. Figure 6 also shows a comparison of the experimental data and the rule-of-mixtures given by:

$$S_{b,f}/S_{b,m} = \rho_f/\rho_m \quad (1)$$

where

$S_{b,f}$ = stress at yield of the foam, MPa
$S_{b,m}$ = stress at yield of the matrix material, MPa
ρ_f = density of the foam, g/cm³
ρ_m = density of the matrix material, g/cm³

The rule-of-mixtures slightly overpredicts the experimental data normalized with respect to the control-2 properties for all of the relative densities explored. Thus, the rule-of-mixtures can be used to estimate the tensile strength of microcellular PC if the properties of the saturation cycled, but unfoamed material are used for normalization. Note that if the tensile strength of the original, unfoamed material (control-1) is used, the rule-of-mixtures significantly overpredicts the tensile strength of the foams.

Figure 7 compares of the tensile strength of microcellular PC normalized by the tensile strength of the original, unprocessed PC (control-1) with several other non-microcellular in-

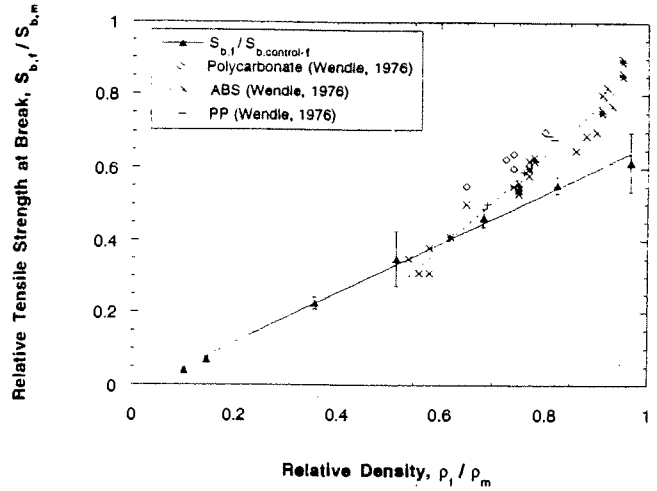

Fig. 7 Comparison of the tensile strength at break of microcellular PC and some common integral foams

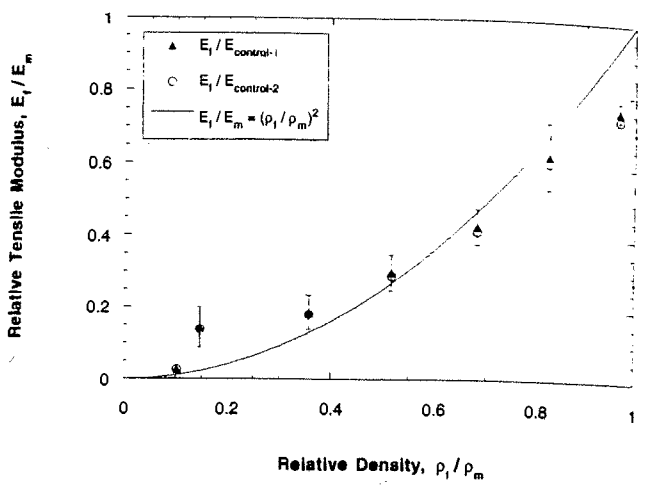

Fig. 8 Plot of the relative yield strength of microcellular PC as a function of the foam relative density, normalized by the yield strength of the original unprocessed PC (control-1) and saturation cycled, but unfoamed PC (control-2)

tegral foams. The relative tensile strength of microcellular PC is approximately equal to the relative tensile strength of other non-microcellular integral foams for relative densities between 0.5 and 0.7, but is lower than the relative tensile strength of the other integral foams above a relative density of 0.7. It should be noted that the traditional integral foams cannot be manufactured below a thickness of approximately 3.2 mm (Shutov, 1986), due to excessive loss of strength. The microcellular specimens tested in this experiment were all under 3.3 mm thick as reported in Table 2. Thus, microcellular foams can be produced at thicknesses below that feasible for non-microcellular integral foams while maintaining strength comparable to the traditional integral foams. Also note from Fig. 7 that the strength of non-microcellular integral foams drops at a faster rate than microcellular PC as the foam density decreases. Table 5 lists the percent elongation at break for the relative densities explored. The relative elongation at break decreases with decreasing relative density, but the trend in this data is not as clear as the trends in the other material properties.

Figure 8 is a plot of the relative yield strength normalized by control-1 and control-2 yield strength as a function of the relative density. Recall that the yield strength is defined as the engineering stress at which the slope of the engineering stress-strain curve becomes zero. As can be seen from Fig. 3, this definition of the yield point is applicable only for foams with a relative density of 0.5 and higher. Lower density foams do not exhibit a hump, or a point of zero slope, in their stress-strain curves. Figure 8 shows that the relative tensile stress at yield decreases linearly with relative density for relative densities of 0.5 and higher.

Figure 9 is a plot of the relative tensile modulus as a function of the relative density. Because there was very little difference between the tensile modulus of the control-1 and control-2 specimens, the foam relative modulus for both controls are approximately equal. Figure 9 shows that a foam with a relative density of 97 percent retains only 76 percent of its stiffness. Thus at higher relative densities, small decreases in density lead to large decreases in stiffness. This significant drop in the modulus implies that foaming affects the modulus of the foam matrix material. At a relative density of 0.15, the relative modulus of the foam is 0.14. Therefore, at low relative densities, the foam appears to be more efficient since the drop in relative modulus is approximately equal to the decrease in relative density.

Figure 9 also shows a comparison of the experimental relative modulus data and the line

$$E_f/E_m = (\rho_f/\rho_m)^2 \qquad (2)$$

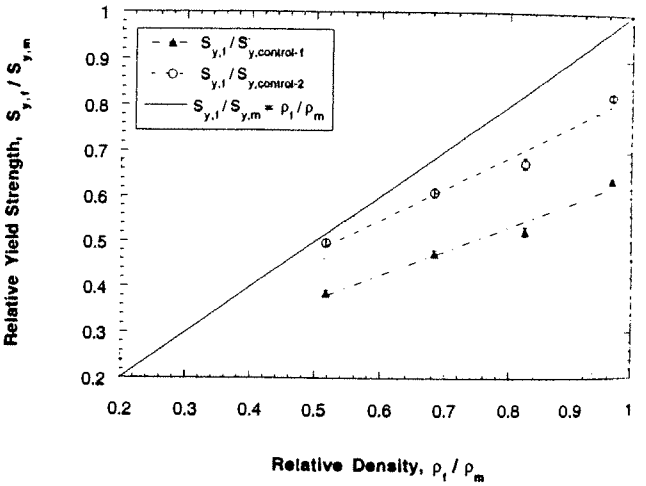

Fig. 9 Plot of the relative foam modulus as a function of the relative density. Note: the tensile moduli of the original, unprocessed PC (control-1) and the saturation cycled, but unfoamed PC (control-2) are approximately equal.

where

E_f = modulus of the foam, MPa
E_m = modulus of the matrix, MPa
ρ_f = density of the foam, g/cm^3
ρ_m = density of the matrix material, g/cm^3

Gibson and Ashby (1988) suggest that the tensile modulus of most foams can be modeled using Eq. (2). The agreement between Eq. (2) and the experimental data is excellent between the relative densities of 0.1 and 0.8. Above a relative density of 0.8, Eq. (2) overpredicts the experimental data. However, further investigation of the tensile modulus of the foams in this range is required before agreement with any model can be discussed.

Conclusions

1. The sorption/desorption cycle of the microcellular process induces a substantial drop in all of the tensile properties of PC except modulus. The ultimate properties of the saturation cycled, but unfoamed PC are approximately 20 percent below the properties of the unprocessed material, even though the CO_2 completely desorbed before testing. Thermal cycling of the original, unprocessed material to the temperatures em-

ployed by the microcellular process does not affect any of the tensile properties. In view of these results, the effect of the gas saturation cycle on the mechanical properties of the polymer should always be considered when characterizing and modelling the microcellular foam mechanical properties.

2. Tensile strength at break as well as yield strength of microcellular PC foams are directly proportional to the foam density. Further, the yield strength is no more than 15 percent less than the tensile strength at break of the foam for a given density. The rule-of-mixtures can provide a good estimate of the tensile strength of microcellular PC if the properties of the saturation cycled, but unfoamed material are used for normalization. The relative modulus of microcellular PC varies as the square of the relative foam density.

3. Microcellular foams with relative densities in the 0.3 to 0.5 range are novel materials offering properties not previously available. Futher, microcellular foams can be produced in thicknesses in the range of 0.5 to 3 mm in which the common structural foams can not be produced due to excessive loss of strength.

The tensile strength of microcellular PC foams is comparable to the tensile strength of common structural foams at equivalent relative densities. However, the strength of structural foams drops at a faster rate than microcellular polycarbonate foam strength as the foam relative density decreases. The relative yield strength of microcellular PC was observed to be five to ten times greater than the relative yield strength of other foams of comparable relative density.

Acknowledgments

This research was primarily supported by the National Science Foundation grant no. MSS 9114840. Partial support was provided by the Washington Technology Centers, the University of Washington-Industry Cellular Composites Consortium, and the Dana Foundation. This support is gratefully acknowledged.

References

Annual Book of ASTM Standards, 1989, Vol 08.01, American Society for Testing and Materials, Philadelphia, PA, pp. 156-167, 299-302.

Baldwin, D. F., and Suh, N. P., 1992, "Microcellular Poly(ethylene terephthalate) and Crystallizable Poly(ethylene terephthalate): Characterization of Process Variables," *SPE Technical Papers*, Vol. 38, pp. 1503-1507.

Brown, N., 1986, *Failure of Plastics*, Brostow, W. and Corneliussen, R. D., eds., Hanser Publishers, New York, pp. 98-101.

Chan, A. H., 1978, "Effect of Annealing Below the Glass Transition on Sorption of Carbon-Dioxide in Polycarbonate," Ph.D. thesis, University of Texas at Austin.

Chan, A. H., and Paul, D. R., 1979, "Influence of History of the Gas Sorption, Thermal and Mechanical Properties of Glassy Polycarbonate," *Journal of Applied Polymer Science*, Vol. 24, pp. 1539-1550.

Colton, J., and Suh, N. P., 1987a, "Nucleation of Microcellular Foam with Additives: Part I: Theoretical Considerations," *Polymer Engineering and Science*, Vol. 27, pp. 485-492.

Colton, J., and Suh, N. P., 1987b, "Nucleation of Microcellular Foam with Additives: Part II: Experimental Results and Discussion," *Polymer Engineering and Science*, Vol. 27, pp. 493-499.

Gibson, L. G., and Ashby, M. F., 1988, *Cellular Solids: Structure and Properties*, Pergamon Press, New York.

Kumar, V., 1988, "Process Synthesis for Manufacturing Microcellular Thermoplastic Parts," Ph.D. thesis, Department of Mechanical Engineering, Massachusetts Institute of Technology, Cambridge, MA.

Kumar, V., and Gebizlioglu, O. S., 1991, "Carbon Dioxide Inducted Crystallization in PET Foams," *SPE Technical Papers*, Vol. 37, pp. 1297-1299.

Kumar, V., and Suh, N. P., 1990, "A Process for Making Microcellular Thermoplastic Parts," *Polymer Engineering & Science*, Vol. 30, pp. 1323-1329.

Kumar, V., and Weller, J. E., 1991, "Microcellular Polycarbonate Part I: Experiments on Bubble Nucleation and Growth," *SPE Technical Papers*, Vol. 37, pp. 1406-1410.

Kumar, V., and Weller, J. E., 1992, "Creating an Integral, Unfoamed Skin on Microcellular Foams," *SPE Technical Papers*, Vol. 38, pp. 1508-1513.

Kumar, V., and Weller, J. E., 1993, "A Process to Produce Microcellular PVC," *International Polymer Processing*, Vol. 8, pp. 73-80.

Kweeder, J. A., Ramesh, N. S., Campbell, G. A., and Rasmussen, D. H., 1991, "The Nucleation of Microcellular Polystyrene Foam," *SPE Technical Papers*, Vol. 37, pp. 1398-1400.

Martini, J. E., Suh, N. P., and Waldman, F. A., 1984, US Patent No. 4,473,665.

Martini, J. E., Waldman, F. A., and Suh, N. P., 1982, "The Production and Analysis of Microcellular Thermoplastic Foams," *SPE Technical Papers*, Vol. 28, pp. 674-676.

Ramesh, N. S., Kweeder, J. A., Rasmussen, D. H., and Campbell, G. A., 1992, "An Experimental Study of the Nucleation of Microcellular Foams in High Impact Polystyrene," *SPE Technical Papers*, Vol. 38, pp. 1078-1081.

Shutov, F. A., 1986, *Integral/Structural Polymer Foams*, Springer-Verlag, New York, p. 4.

Weller, J. E., 1991, "Synthesis of a Manufacturing Process for Making Microcellular Polycarbonate Parts," M.S. thesis, University of Washington, Seattle, Washington.

Wendle, B. C., 1976, *Engineering Guide to Structural Foam*, Technomic, Westport, CT, p. 93.

(Contents continued)